

## Magnitude-tunable sub-THz shear phonons in a non-polar GaN multiple-quantum-well p-i-n diode

Chien-Cheng Chen, Hwei-Min Huang, Tien-Chang Lu, Hao-Chung Kuo, and Chi-Kuang Sun

Citation: *Applied Physics Letters* **100**, 201905 (2012); doi: 10.1063/1.4718524

View online: <http://dx.doi.org/10.1063/1.4718524>

View Table of Contents: <http://scitation.aip.org/content/aip/journal/apl/100/20?ver=pdfcov>

Published by the *AIP Publishing*

---

### Articles you may be interested in

The effect of silicon doping in the barrier on the electroluminescence of InGaN/GaN multiple quantum well light emitting diodes

*J. Appl. Phys.* **114**, 103102 (2013); 10.1063/1.4820450

Influence of residual oxygen impurity in quaternary InAlGaN multiple-quantum-well active layers on emission efficiency of ultraviolet light-emitting diodes on GaN substrates

*J. Appl. Phys.* **99**, 114509 (2006); 10.1063/1.2200749

Ultra-low-frequency self-oscillation of photocurrent in  $\text{In}_x\text{Ga}_{1-x}\text{As}/\text{Al}_{0.15}\text{Ga}_{0.85}\text{As}$  multiple-quantum-well p-i-n diodes

*Appl. Phys. Lett.* **85**, 3483 (2004); 10.1063/1.1806268

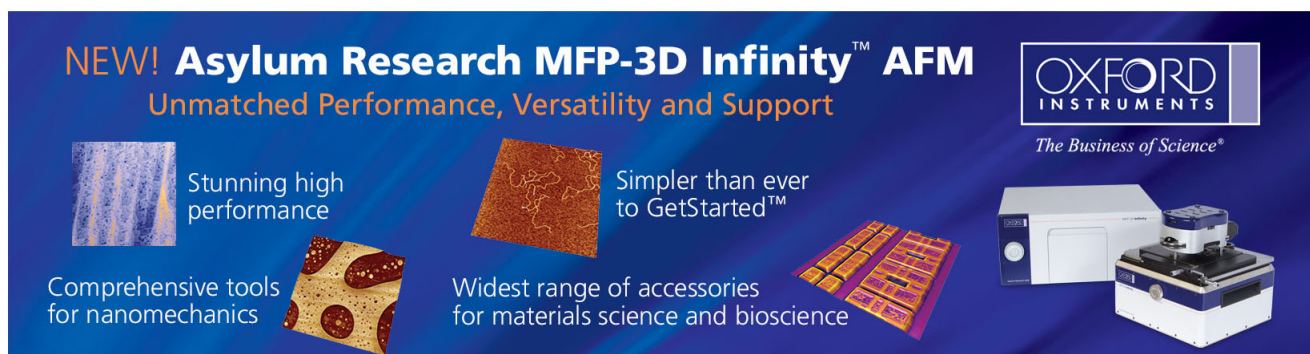
InGaN multiple-quantum-well green light-emitting diodes on Si grown by metalorganic chemical vapor deposition

*J. Appl. Phys.* **91**, 528 (2002); 10.1063/1.1408264

GaN/GaN multiple-quantum-well light-emitting diodes grown by molecular beam epitaxy

*Appl. Phys. Lett.* **74**, 3616 (1999); 10.1063/1.123199

---



**NEW! Asylum Research MFP-3D Infinity™ AFM**  
Unmatched Performance, Versatility and Support

**OXFORD INSTRUMENTS**  
*The Business of Science®*

Stunning high performance  
Simpler than ever to GetStarted™  
Comprehensive tools for nanomechanics  
Widest range of accessories for materials science and bioscience

The advertisement features several images: a blue textured surface, a brown textured surface, a grid of colorful rectangular samples, and the Asylum Research MFP-3D Infinity AFM instrument.

# Magnitude-tunable sub-THz shear phonons in a non-polar GaN multiple-quantum-well p-i-n diode

Chien-Cheng Chen,<sup>1</sup> Huei-Min Huang,<sup>2</sup> Tien-Chang Lu,<sup>2</sup> Hao-Chung Kuo,<sup>2</sup> and Chi-Kuang Sun<sup>1,3,a)</sup>

<sup>1</sup>Department of Electrical Engineering and Graduate Institute of Photonics and Optoelectronics, National Taiwan University, Taipei 10617, Taiwan

<sup>2</sup>Department of Photonics and Institute of Electro-Optical Engineering, National Chiao Tung University, Hsinchu 300, Taiwan

<sup>3</sup>Institute of Physics, Academia Sinica, Taipei 115, Taiwan and Molecular Imaging Center, National Taiwan University, Taipei 10617, Taiwan

(Received 2 February 2012; accepted 1 May 2012; published online 15 May 2012)

Coherent transverse acoustic phonons are optically generated and detected through the piezoelectric coupling between the build-in electric fields and shear strains of a non-polar GaN multiple quantum wells embedded in a p-n junction. By optical transient transmission change measurement, the phonon frequency is observed to be 0.4 THz which corresponds to a wavelength of 12.5 nm, the periodicity of the multiple quantum wells, and the estimated phonon velocity corresponds to the transverse acoustic phonon velocity in GaN. Moreover, we can magnify the driving amplitude of the generated shear phonons by increasing the reverse bias of the p-i-n diode.

© 2012 American Institute of Physics. [<http://dx.doi.org/10.1063/1.4718524>]

Coherent acoustic phonons with frequencies in the THz regime, corresponding to wavelengths in the nano-meter range, have long been interested<sup>1-12</sup> for their wide applications in diagnostics of nanostructures<sup>3-5</sup> as well as ultrafast optical,<sup>6</sup> electronic,<sup>7</sup> and magnetic modulations.<sup>8</sup> Exciting materials by ultrashort laser pulses provides an elegant method to generate and subsequently observe coherent acoustic phonons without the need of a cryogenic environment and permits the investigation of material properties at room temperature.<sup>9-12</sup> However, in most experiments the generated coherent phonons were limited to longitudinal acoustic (LA) phonons because of the lateral symmetry of the excited crystal. Although LA phonons can convert to transverse acoustic (TA) mode by diffraction, the fact that the beam spots of the acoustic waves are much larger than the pulse widths makes laser-excited coherent phonons quasi-plane waves and keeping in LA mode.<sup>13</sup>

Coherent TA phonons are not only complementary to LA phonons but also of special interests in diagnostics of nanostructures or molecular systems in which shear responses are more important than the dilatational ones.<sup>3</sup> In 2000 Hurely *et al.*<sup>13</sup> reported the mode conversion from LA to TA phonons after reflected from an isotropic-anisotropic crystal interface and then motivated direct TA phonon generations by exciting crystals with asymmetrically cut surfaces<sup>14,15</sup> and superlattices grown along asymmetric axes.<sup>14,16,17</sup> In addition, TA phonons converted from LA phonons have also been manifested by tightly focusing laser beam on a sub-micrometric metallic transducer to violate the unidirectionality of phonon propagation.<sup>18</sup> Recently, breathing confined acoustic vibrations of metallic nanodisk have also been utilized to generate shear acoustic waves with frequency controlled by the size of the disks.<sup>19</sup> Nevertheless, in

most of these experiments the magnitudes of TA phonons were weaker than that of the simultaneously generated LA phonons. This problem together with the poor sensitivity of probing TA phonons<sup>20,21</sup> makes the applications of TA phonons difficult.

Recently, we have optically observed backward Brillouin oscillations resulted from coherent TA and LA phonons generated by piezoelectric effect and deformation coupling, respectively, in non-polar bulk GaN.<sup>22</sup> The magnitude of TA phonons has been shown to be able to highly exceed the magnitude of LA phonons by lowering the pump fluence. Motivated by our previous successes,<sup>12,22</sup> in this work we fabricated multiple quantum wells (MQWs) grown in  $[1\bar{1}00]$  direction to generate sub-THz coherent TA phonons. By optical transient transmission change measurement, the phonon frequency was observed to be as high as 0.4 THz. With the MQWs periodicity accurately measured by high-resolution x-ray diffraction, the velocity of the generated TA phonons was estimated to be 4880 m/s, which agrees reasonably well with the reported 4240 m/s velocity of TA phonons in GaN.<sup>22</sup> Most importantly, the driving amplitude of the TA phonons can be enhanced by raising the reverse bias across the p-i-n junction where the MQWs lie in.

For the wurtzite GaN with 6 mm symmetry,<sup>23</sup> the non-vanishing piezoelectric constants are  $e_{33}$ ,  $e_{32}(=e_{31})$ , and  $e_{24}(=e_{15})$ . In matrix notation, the relation between polarization field  $\mathbf{P}$  and strain  $\mathbf{s}$  can be expressed by

$$\begin{bmatrix} P_1 \\ P_2 \\ P_3 \end{bmatrix} = \begin{bmatrix} 0 & 0 & 0 & 0 & e_{15} & 0 \\ 0 & 0 & 0 & e_{24} & 0 & 0 \\ e_{31} & e_{32} & e_{33} & 0 & 0 & 0 \end{bmatrix} \begin{bmatrix} s_1, s_2, s_3, s_4, s_5, s_6 \end{bmatrix}^T. \quad (1)$$

For the MQWs grown along c-axis ( $[0001]$ ), there are static polarization field,  $P_3$ , induced by strong static strains resulted from lattice mismatch between InGaN and GaN.

<sup>a)</sup>Author to whom correspondence should be addressed. Electronic mail: [sun@cc.ee.ntu.edu.tw](mailto:sun@cc.ee.ntu.edu.tw).

As the MQWs were excited by femtosecond laser pulses, the static strain would be lunched because of the instantaneous screening of  $P_3$  by separately photo-generated electrons and holes.<sup>12</sup> The spontaneous polarization field,  $P_3$ , can only piezoelectrically couple to dilatational strains,  $s_1$ ,  $s_2$ , and  $s_3$ . To manifest shear strains,  $s_4$ ,  $s_5$ , and  $s_6$ , we have to grow MQWs along some other directions so that  $e_{24}$  or  $e_{15}$  can be involved in the piezoelectric effect.

A macroscopic load-string model has been presented in Ref. 24 to study the effect of crystal orientation of GaN MQWs on the magnitudes of LA and TA phonons. In wurtzite GaN, piezoelectric effect and deformation potential coupling are the two main mechanisms to generate acoustic phonons. Deformation potential coupling will only contribute to the generation of LA phonons, so we can neglect it in the TA phonon generations. On the other hand, the piezoelectric driving forces for the LA and TA modes can be expressed by<sup>24</sup>

$$f_{\lambda, \text{piezo}} = -\frac{\bar{e}_{\lambda}}{\bar{\epsilon}} \rho_{SC}, \quad (2)$$

where  $\rho_{SC} = \rho_h - \rho_e$  is the space charge defined by the density difference of holes and electrons,  $\bar{\epsilon} = \epsilon_{kl} n_k n_l$  is the effective dielectric constant along propagation direction, and  $\bar{e}_{\lambda} = e_{ijk} n_i n_j \hat{w}_{\lambda, k}$  is the effective piezoelectric constants with  $\lambda = \text{LA}$  and  $\text{TA}$ ,  $e_{ijk}$  is the piezoelectric tensor of GaN,  $\hat{n}$  is the unit vector of phonon propagating direction, and the unit vectors  $\hat{w}_{\lambda}$  indicate the polarization directions of  $\lambda$  modes. Equation (2) is derived from elastic wave equation and Maxwell's equation under the assumption that the elastic and dielectric properties of barriers and wells are the same. Also note that the  $f_{\lambda, \text{piezo}}$  can only be decomposed into two phonon polarization directions on the plane spanned by  $\hat{n}$  and  $\hat{x}_3$ , because the projection of  $f_{\lambda, \text{piezo}}$  into the third polarization direction normal to the plane is always zero. Since wurtzite GaN is uniaxial, it is sufficient to describe phonon propagating direction by an angle  $\theta$  between  $\hat{n}$  and  $\hat{x}_3$ . More specifically, with the Cartesian coordinate as shown in Fig. 1(a), the effective piezoelectric constants for LA and TA modes can be expressed as<sup>22,24</sup>

$$\bar{e}_{LA} = [(2e_{24} + e_{32})\sin^2\theta + e_{33}\cos^2\theta]\cos\theta, \quad (3)$$

$$\bar{e}_{TA} = [(e_{24} + e_{32} + e_{33})\cos^2\theta - e_{24}\sin^2\theta]\sin\theta \quad (4)$$

respectively. Therefore, MQWs grown along the direction with an orientation angle  $\theta = 90^\circ$  will be a suitable candidate to achieve pure TA phonon generations by piezoelectric effect.

An m-plane ( $\theta = 90^\circ$ )  $\text{In}_{0.22}\text{Ga}_{0.78}\text{N}/\text{GaN}$  p-i-n diode similar to the one investigated in Ref. 25 was fabricated to generate coherent TA phonons in this work. As depicted in Fig. 1(b), the 6-pair MQWs were sandwiched by a p- and a n-doped GaN to form a p-i-n structure. The spatial period  $D$  of the MQWs was determined by the high-resolution x-ray diffraction, as displayed in Fig. 1(c). Through the formula  $D = \lambda/2\Delta\Theta$ , where  $\lambda$  is the wavelength of the x-ray and  $\Delta\Theta$  is the angle difference between the diffraction peaks, the period  $D$  of MQWs was found to be 12.2 nm with  $\lambda = 0.154$  nm and  $\Delta\Theta = 6.3 \times 10^{-3}$  rad. The doping densities of p-doped and n-doped GaN are  $1 \times 10^{18} \text{ cm}^{-3}$  and  $5 \times 10^{18} \text{ cm}^{-3}$ , respectively. The resulting built-in voltage is around 2.1 V and the depletion region is 179-nm thick. The p-i-n structure provides a built-in electric field along  $x_2$ -axis,  $P_2$ , within the depletion region and induces an in-plane static shear stress,  $s_4$ . According to the doping densities, the built-in electric field was estimated to be 120 kV/cm, and the induced shear strain is around  $10^{-5}$ . This shear strain can be launched as soon as the built-in electric field was screened by the photocarriers excited by femtosecond laser pulses. In this scheme the acoustic wave will have the same periodicity as the MQWs,<sup>12,24</sup> so the wavelength of the phonons,  $\lambda_{\text{phonon}}$ , will equal to  $D$ . As propagating through the quantum wells, the generated shear waves will affect the electric field along the epitaxial direction inside and induce variations in the optical transmission. The frequency of the induced oscillation in the optical transmission change will then equal to the inverse of the travelling time of the strain pulse from one quantum well to the adjacent one.<sup>12,24</sup>

Optical transient transmission change measurement<sup>12</sup> was used to observe the phonon oscillation. The output beam emitted from mode-locked Ti:Sapphire laser (Coherent, Mira 900F) was first frequency-doubled by a beta barium borate (BBO) crystal to a wavelength of 455 nm to selectively excite the  $\text{In}_{0.22}\text{Ga}_{0.78}\text{N}$ . After second harmonic generation, the laser beam passed through a blue colour filter and a half-wave plate to selectively block the remaining 800 nm-wavelength component and to control the polarization direction, respectively. The laser beam was then separated by a polarizing beam splitter into the excitation and

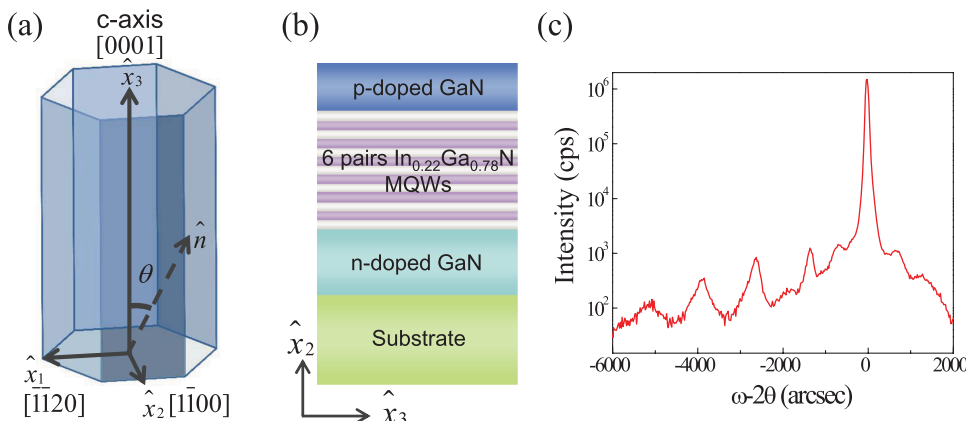


FIG. 1. (a) Coordinate adopted to express the effective piezoelectric constants in Eqs. (1)–(4). (b) Schematic diagram of the m-plane p-i-n structure. The epitaxial direction is along  $[1\bar{1}00]$ . (c) X-ray diffraction measurement of the MQWs. The spatial period of the MQWs is estimated to be 12.5 nm.

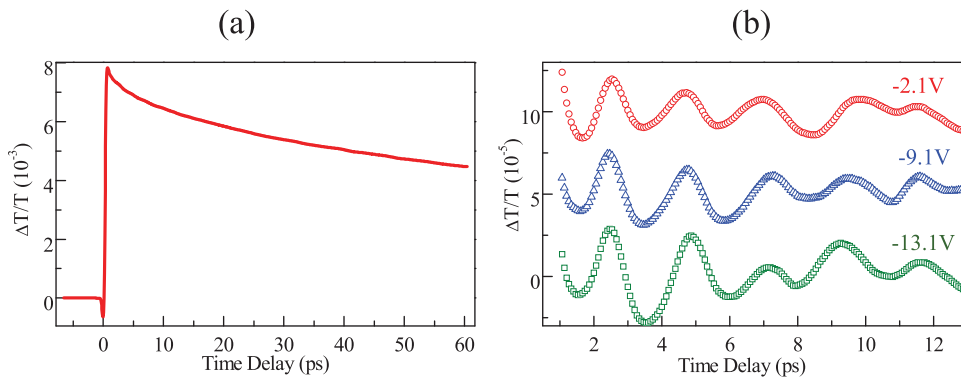


FIG. 2. (a) Measured transmission changes as a function of delay time for the unbiased (with built-in voltage  $-2.1$  V) m-plane p-i-n diode under a pump fluence of  $320 \mu\text{J}/\text{cm}^2$ . (b) Background-removed signals with the voltage jumps of  $-2.1$  V (red circles),  $-9.1$  V (blue triangles), and  $-13.1$  V (olive squares) in former 13 ps to display the TA phonon oscillations.

detection beams whose ratio can be adjusted by rotating the half-wave plate. The transmission change caused by excitation beam was subsequently probed by the detection beam with an optical delay time controlled by a mechanical translational stage. Figure 2(a) shows the transmission changes of the unbiased p-i-n diode as a function of delay time  $t$  under an excitation fluence of  $320 \mu\text{J}/\text{cm}^2$ . The dip at  $t = 0$  is the signal of two-photon absorption resulted by pump and probe photons in the bulk GaN.<sup>26</sup> From the width of this dip, the temporal width of the frequency-doubled laser pulse can be estimated to be 250 fs. Behind the dip is a rapid transmission increase followed by the carrier cooling dynamics. On top of the slowly decaying curve, there are oscillation signal on the order of  $\Delta T/T \sim 10^{-5}$ , which is too weak to be directly visualized in Fig. 2(a). To analyze the oscillation, we subtracted the exponentially decaying background from the signal and zoom in to the 6 periods of oscillation in the initial 13 ps, as shown by the red circles in Fig. 2(b). We can clearly see oscillations with a period  $T$  around 2.5 ps, corresponding to the frequency of 0.4 THz as revealed by the FFT spectrum shown by the red circles in Fig. 3(a). One can notice that the oscillation is sinusoidal type which is a signature of phonon oscillations resulted from piezoelectric effect.<sup>12</sup> The frequency of the phonons generated in MQWs is given by  $f = v/\lambda_{\text{phonon}}$ ,<sup>12</sup> where  $v$  is the phonon velocity. With the observed 0.4 THz frequency and the measured periodicity  $D = 12.2$  nm, we found that the shear phonon velocity in MQWs is 4880 m/s which agrees reasonably with the reported sound velocity,  $v = 4240$  m/s,<sup>22</sup> of the acoustic phonons propagating in the direction normal to and polarized in c-axis of GaN.

The optical detection sensitivity of TA phonons has been known to be much weaker than that of LA phonons and transient polarimetry<sup>20</sup> and time-resolved electron diffrac-

tion<sup>21</sup> have been proposed to enhance the detection of TA phonons. In polar GaN MQWs, the transient transmission change  $\Delta T/T$  induced by LA phonons with a strain amplitude of  $10^{-4}$  is around  $10^{-3}$ ; meanwhile, the  $10^{-5}$  shear strain caused a transient transmission change of  $10^{-5}$  in this work. Hence, the piezoelectric detection sensitivity of TA phonons in nonpolar GaN MQWs is one order smaller than that of LA phonons in polar GaN MQWs. In most experiments,<sup>14–22</sup> the generations of TA phonons were accompanied with the generations of LA phonons. In non-polar GaN, LA phonons have also been shown to be generated through deformation potential coupling.<sup>22</sup> In the theoretical analysis,<sup>24</sup> it has also been shown that there will be deformation-potential-coupled LA phonons with amplitude 5 times lower than that of the piezoelectrically coupled TA phonons in the non-polar GaN MQWs excited by a saturated pump fluence. Although LA phonons cannot be piezoelectrically detected in non-polar GaN, they have chances to be detected through deformation potential coupling.<sup>27</sup> However, in this experiment only TA phonons were observed, and LA phonons were still absent even with a highly saturated pump fluence,  $320 \mu\text{J}/\text{cm}^2$ . This result indicates that the detection sensitivity of LA phonons through deformation potential coupling is trivial in this non-polar GaN MQWs.

In this investigation, the initial shear strains were provided by the built-in electric field of the p-i-n structure. We could thus magnify the amplitude of the observed TA phonon signal by increasing the reverse bias across the junction. The red circles, blue triangles, and olive squares in Fig. 3(a) show the Fourier spectra of the corresponding phonon oscillations shown in Fig. 2(b), which are observed with different biases under the same pump fluence. It can be clearly seen that the TA phonon signal is enhanced as the reverse bias increases. This result not only further validates that the TA phonon

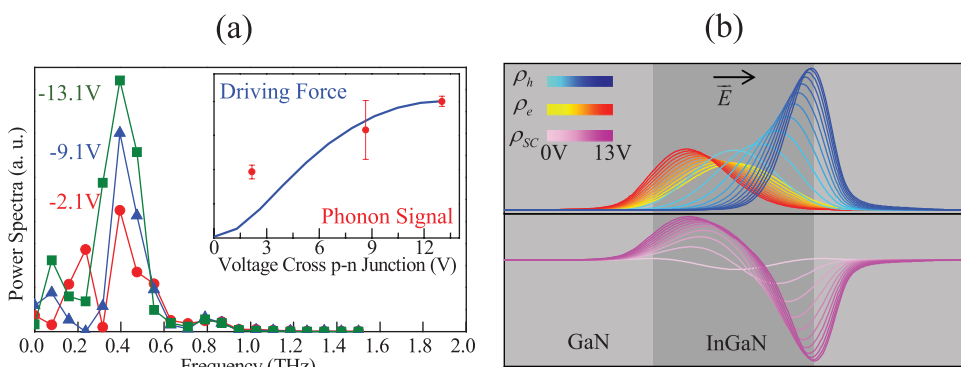


FIG. 3. (a) Corresponding Fourier power spectra of pump probe signal shown in Fig. 2. The red dots in the inset are the pick values of the Fourier power spectra for different voltage jumps. (b) The calculated density distributions of electrons  $\rho_e$ , holes  $\rho_h$ , and space charges  $\rho_{sc}$  in the quantum well with various voltage jumps indicated by the colour bars. The normalized intensity of the corresponding piezoelectric driving forces is displayed by the blue curve in the inset of (a).

generations were through piezoelectric coupling but also shows great application potential of this phonons source.

To further understand this experimental result, we use the macroscopic load-string model<sup>24</sup> to calculate the phonon amplitude for different bias conditions. It can be seen from Eq. (2) that for a given propagation direction the driving force is directly proportional to the space charge density which can be obtained by calculating the wave functions of holes and electrons in the quantum well. Figure 3(b) shows the calculated spatial distributions of electrons, holes, and space charges for different voltage jumps cross the p-n junction. For quantum wells with a zero electric field, the space charge can only be contributed by the difference of effective masses of electrons and holes. As the voltage jump increases, the electrons and holes gradually separate, and the space charge becomes stronger and stronger. The inset of Fig. 3(a) shows the comparison of the measured phonon signals and the calculated driving forces for different voltage jumps. The error bars of the experimental signals are estimated from the magnitudes of the 400 GHz component of the background-removed pump-probe traces behind 13 ps. Also, note that the driving force with a voltage jump of 13 V has been normalized to the phonon signal measured at the same voltage jump. The deviation of the experimental and calculated results may be resulted from the suppression of detection sensitivity owing to the applied reverse bias.<sup>28</sup>

In summary, 0.4 THz TA phonons in m-plane GaN MQWs have been generated and detected through piezoelectric coupling. The phonon signals have been shown to be magnified by means of increasing the reverse bias, despite the suppression of detection sensitivity. Our result demonstrated the great application potential of non-polar GaN MQWs in THz shear acoustics.

The authors would like to thank Dr. Yu-Chieh Wen and Professor Vitalyi Gusev for stimulating discussions. This work was sponsored by National Science Council of Taiwan under Grant No. 100-2120-M-002-009.

<sup>1</sup>H. Kinder, *Phys. Rev. Lett.* **28**, 1564 (1972).

<sup>2</sup>P. Berberich, R. Buemann, and H. Kinder, *Phys. Rev. Lett.* **49**, 1500 (1982).

<sup>3</sup>T. Pezeril, C. Klieber, S. Andrieu, and K. A. Nelson, *Phys. Rev. Lett.* **102**, 107402 (2009).

- <sup>4</sup>A. Steigerwald, Y. Xu, J. Qi, J. Gregory, X. Liu, J. K. Furdyna, K. Varga, A. B. Hmelo, G. Lüpke, L. C. Feldman, and N. Tolk, *Appl. Phys. Lett.* **94**, 111910 (2009).
- <sup>5</sup>C. Mechri, P. Ruello, J. M. Breteau, M. R. Baklanov, P. Verdonck, and V. Gusev, *Appl. Phys. Lett.* **95**, 091907 (2009).
- <sup>6</sup>T. Berstermann, C. Bruggemann, M. Bombeck, A. V. Akimov, D. R. Yakovlev, C. Kruse, D. Hommel, and M. Bayer, *Phys. Rev. B* **81**, 085316 (2010).
- <sup>7</sup>D. M. Moss, A. V. Akimov, B. A. Glavin, M. Henini, and A. J. Kent, *Phys. Rev. Lett.* **106**, 066602 (2011).
- <sup>8</sup>A. V. Scherbakov, A. S. Salasyuk, A. V. Akimov, X. Liu, M. Bombeck, C. Bruggemann, D. R. Yakovlev, V. F. Sapega, J. K. Furdyna, and M. Bayer, *Phys. Rev. Lett.* **105**, 117204 (2010).
- <sup>9</sup>C. Thomsen, J. Strait, Z. Vardeny, H. J. Maris, J. Tauc, and J. J. Hauser, *Phys. Rev. Lett.* **53**, 989 (1984).
- <sup>10</sup>A. Bartels, T. Dekorsy, H. Kurz, and K. Köhler, *Phys. Rev. Lett.* **82**, 1044 (1999).
- <sup>11</sup>O. B. Wright, *Phys. Rev. B* **49**, 9985 (1994).
- <sup>12</sup>C.-K. Sun, J.-C. Liang, and X.-Y. Yu, *Phys. Rev. Lett.* **84**, 179 (2000).
- <sup>13</sup>D. H. Hurley, O. B. Wright, O. Matsuda, V. E. Gusev, and O. V. Kolosov, *Ultrasonics* **38**, 470 (2000).
- <sup>14</sup>O. Matsuda, O. B. Wright, D. H. Hurley, and V. E. Gusev, and K. Shimizu, *Phys. Rev. Lett.* **93**, 095501 (2004).
- <sup>15</sup>T. Pezeril, P. Ruello, S. Gougeon, N. Chigarev, D. Mounier, J.-M. Breteau, P. Picart, and V. Gusev, *Phys. Rev. B* **75**, 174307 (2007).
- <sup>16</sup>R. N. Kini, A. J. Kent, N. M. Stanton, and M. Henini, *Appl. Phys. Lett.* **88**, 134112 (2006).
- <sup>17</sup>P. Walker, R. P. Campion, A. J. Kent, D. Lehmann, Cz. Jasiukiewicz, *Phys. Rev. B* **78**, 233307 (2008).
- <sup>18</sup>C. Rossignol, J. M. Rampnoux, M. Perton, B. Audoin, and S. Dilhaire, *Phys. Rev. Lett.* **94**, 166106 (2005).
- <sup>19</sup>A. Amziane, L. Belliard, F. Decremps, and B. Perrin, *Phys. Rev. B* **83**, 014102 (2011).
- <sup>20</sup>D. Mounier, P. Picart, P. Babilotte, P. Ruello, J.-M. Breteau, T. Pezeril, G. Vaudel, M. Kouyaté, and V. Gusev, *Opt. Express* **18**, 6767 (2010).
- <sup>21</sup>M. Harb, W. Peng, G. Sciaini, C. T. Hebeisen, R. Ernstorfer, M. A. Eriksson, M. G. Lagally, S. G. Kruglik, and R. J. D. Miller, *Phys. Rev. B* **79**, 094301 (2009).
- <sup>22</sup>Y.-C. Wen, T.-S. Ko, T.-C. Lu, H.-C. Kuo, J.-I. Chyi, and C.-K. Sun, *Phys. Rev. B* **80**, 195201 (2009).
- <sup>23</sup>J. F. Nye, *Physical Properties of Crystals* (Oxford University Press, Oxford, 1957).
- <sup>24</sup>G.-W. Chern, C.-K. Sun, G. D. Sanders, and C. J. Stanton, in *Ultrafast Dynamical Processes in Semiconductors*, edited by K.-T. Tsen (Springer, Berlin/Heidelberg, 2004).
- <sup>25</sup>S.-C. Ling, T.-C. Lu, S.-P. Chang, J.-R. Chen, H.-C. Kuo, and S.-C. Wang, *Appl. Phys. Lett.* **96**, 231101 (2010).
- <sup>26</sup>C.-K. Sun, J.-C. Liang, J.-C. Wang, F.-J. Kao, S. Keller, M. P. Mack, U. Mishra, and S. P. DenBaars, *Appl. Phys. Lett.* **76**, 439 (2000).
- <sup>27</sup>D. M. Moss, A. V. Akimov, A. J. Kent, B. A. Glavin, J. Kappers, J. L. Hollander, M. A. Moram, and C. J. Humphreys, *Appl. Phys. Lett.* **94**, 011909 (2009).
- <sup>28</sup>P.-H. Wang, Y.-C. Wen, S.-H. Guol, C.-M. Lai, H.-C. Lin, P.-R. Chen, J.-W. Shi, J.-I. Chyi, and C.-K. Sun, *Appl. Phys. Lett.* **95**, 143108 (2009).